Egyptian Journal of Chemistry

http://ejchem.journals.ekb.eg/

Efficient CPE-ICP OES Determination of Palladium (II) in Environmental Samples Using Schiff Base Ligand and Triton X-114

Menna K. Nour, Magdy Y. Abdelaal and Magda A. Akl *

Chemistry Department, Faculty of Science, Mansoura University, Mansoura 35516, Egypt

Abstract

In this study, a conjugated methodology of both cloud point extraction and inductively coupled plasma optical emission spectroscopy (CPE-ICP-OES) was employed for the ultra-trace determination of Pd^{2+} in various environmental samples. The N, N'-(1, 2-phenylene) bis (3-amino benzamide Schiff base, (A_1) was utilized to form red colored [Pd^{II}-(A_1)$_2$] complex, at pH 4. Initially, the complex was isolated in the surfactant-rich layer by applying a nonionic surface-active agent, Triton X-114. Furthermore, the surfactant-rich layer was eluted using 3 mol/L HNO_3 and the concentration of Pd^{2+} was, then, determined using ICP-OES. The different experimental variables affecting the CPE were investigated as the solution acidity, the concentration of metal ion, chelating ligand and the surface-active agent, the different types of surface-active agents, temperature, and centrifugation time. The analytical detection limit of Pd^{2+} was found to be 0.02128µg/L, with a pre-concentration factor of 100. The recovery (%) of the Pd^{2+} is >95% and the relative standard deviation (RSD, %) is <1%. The proposed CPE-ICP OES has been successfully applied for the determination of Pd^{2+}in real water samples. The plausible mechanism of interaction between the [Pd^{II}-(A_1)$_2$] complex and TX-114 is elucidated.

Keywords: Schiff bases; TX-114; Cloud point extraction; ICP-OES; Palladium

1. Introduction

In this century, water-related issues have emerged as one of humanity's greatest concerns[1]. The term "water pollution" refers to the disruption of aquatic ecosystems caused by the introduction of foreign substances[2,3]. Because of this, the water becomes toxic, posing a threat to both human and animal life. Hydration is crucial in the cycle of nutrient reuse[4]. Sedimentation, erosion, temperature, and the dumping of oil, grease, detergents, and pesticides down drains, as well as certain nutrients, agricultural activities, and hazardous pollutant agents, are just a few of the many elements that may have a major influence on water quality[5].

Palladium is frequently utilized globally in the industry as it has remarkable chemical and physical characteristics, like its high corrosion resistance, stability in its thermoelectricity, and its activity as a catalyst[6]. The electronic industry, the production of dental and medical equipment, the chemical processes of hydrogenation, dehydrogenation, and organic synthesis, and the development of automobile catalytic converters are just some of the many industries in which palladium has found considerable application[7]. Currently, it is anticipated that the production of auto catalysts consumes more than fifty percent of the world's yearly palladium output[8]. The elevated palladium consumption in several industrial sectors has remarkably raised pollution caused by palladium[9].

Methylated processes in aquatic environments were thought to be enhanced by palladium and that, by applying the suitable conditions, it might become concentrated in the food chain, causing threats to ecosystems and human health[10]. Hence, it is vital to develop a strategy for detecting palladium traces in water samples that is necessarily rapid, dependable, and precise. The matrix effects and/or the low palladium concentration make it difficult to acquire precise results using conventional analytical strategies. To overcome these difficulties, pre-concentration and separation methodologies are used [11] such as Adsorption[12–24], LLE(liquid-liquid extraction)[25], co-precipitation[26], column extraction[27], ISE(ion-selective electrode)[28], flotation[29–31] and CPE(cloud point extraction)[28]. The cloud point extraction technique has many advantages over other methods. It is quick, simple to

*Corresponding author e-mail: magdaakl@yahoo.com.; (Magda A Akl).

Receive Date: 15 February 2023, **Revise Date:** 20 March 2023, **Accept Date:** 23 March 2023,
First Publish Date: 25 March 2023
DOI: 10.21608/EJCHEM.2023.194183.7614

use, and environmentally friendly[32] and it also uses non-toxic surfactants[33].

ICP-OES was used for the identification of divalent Pd traces after its pre-concentration using a chelating agent[34]. There have been raising interest in the use of chelating agents as hydrophobic extracting agents in the isolation of trace metal ions[35]. Using CPE, large amounts of sample fluids may be isolated from inorganic ions. In coordination chemistry, Schiff bases may act as a starting point for designing a wide range of ligand complexes that can bind to metal ions in tunable methods[35,36].

The preparation of the C1 complex (a nano divalent palladium complex with the N, N'-(1, 2-phenylene) bis (3-amino benzamide) Schiff base, A_1 and its characterization has been reported in our recently published work [37].

A review of the literature revealed that the combined CPE-ICP OES determination of palladium(II) is rarely reported using the N, N'-(1, 2-phenylene) bis (3-aminobenzamide) Schiff base ligand (A_1) and Triton X-114 surfactant.

In this study, pre-concentration and determination of Pd(II) traces in variable environmental water samples through CPE ICPOES methodology have been employed. In this study, Pd(II) was preconcentrated and separated using A_1 as a chelating ligand and TX-114 nonionic surfactant followed by ICP OES determination. The parameters affecting the CPE of Pd(II) were thoroughly investigated *viz.* the influence of solution acidity, the influence of metal ion and chelating ligand concentration, the influence of surface-active agent concentration, the influence of different types of surface-active agents, temperature influence, centrifugation time and rate influence, foreign ions influence and volume influence were studied.

2. Experimental

2.1. Reagents and solutions

All the chemicals used in this work were of analytical-reagent grade, and doubly distilled water (DDW) was used. Palladium(II) chloride hydrated $PdCl_2.2H_2O$ was obtained from Sigma Aldrich. Different stock solutions were prepared. 1×10^{-4}mol/L Pd (II) stock solution was obtained by dissolving 0.00106 g $PdCl_2.2H_2O$ in 100 ml DDW in the presence of 1.0 ml conc. HCL. Stock solution of the Schiff base (A_1) (1×10^{-3}mol/L) was prepared by dissolving 0.04385 g (A_1) in 100 ml of ethanol. Without additional purification, the non-ionic surfactant TX-114 from Sigma Aldrich was employed, scheme 1. A stock solution of TX-114 at 1% (v/v) was created by dissolving 1 mL of TX-114 in 5 mL of ethanol and adding 100 ml DDW.

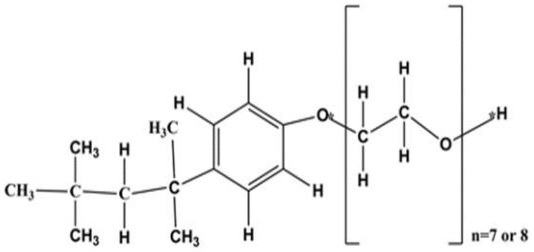

Scheme1: Triton X-114 structure.

2.2. Instrumentation

Using KBr tablets and a JASCO FT/IR-460 spectrophotometer at room temperature, the FT-IR spectra were reported in the 400–4000 cm^{-1} range. Using a PerkinElmer 550 Spectrophotometer and a 1 cm quartz cell, the UV-Vis spectra of Schiff base (A_1) and the palladium complex (C1) throughout a wavelength range of 200-900 nm, were obtained. An ICP-OES Varian spectrometer Model Varian Vista Pro, CCD Simultaneous was used to determine Pd(II) concentration.

2.3. Preparations

2.3.1. Preparation of the Schiff base ligand (A_1)

In recently published work[38], the Schiff base (A_1) was prepared by the refluxing 3-aminobenzoic acid (3-ABA) (2.0 mmol, 0.2743g) dissolved in 10 ml ethanol with 5 ml of 1, 2-phenylenediamine (Phen) (1.0 mmol, 0.1081 g) dissolved in ethanol in the presence of 2 drops of glacial acetic acid (1mol/L) for 2 days at 75°C according to reaction synthesis scheme 2. The produced reddish-brown precipitate was filtered, washed many times using water/ethanol, and then dried under a vacuum atmosphere. The proposed mechanism of Schiff base ligand (A_1) synthesis is presented in scheme 2 and the 3 D structure of A_1 is presented in scheme 3.

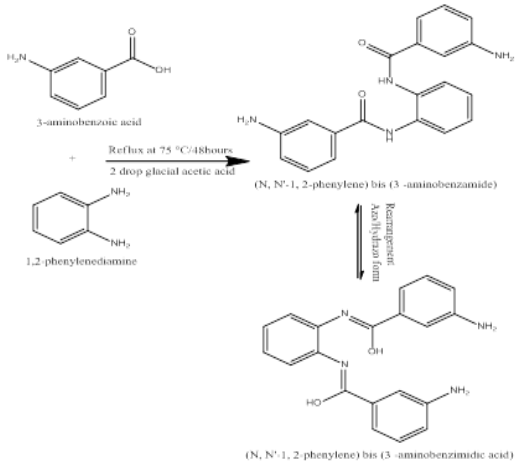

Scheme2: The proposed mechanism of synthesis of the Schiff base ligand (A_1)

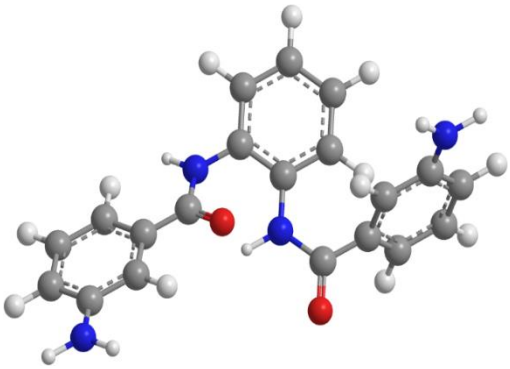

Scheme3: 3D structure of ligand

2.3.2. Preparation of Pd-(A_1) complex

Palladium-A_1 complex (C1) was prepared by refluxing of $PdCl_2.2H_2O$ (1.0 mmol, 0.2134g) dissolved in 10 ml DDW with the Schiff base (A_1) for 2 days at 75° C, relative to reaction synthesis. As the reaction proceeded, the color of the solution shifted from reddish brown to a dark red precipitate. The dark red precipitate was filtered, washed many times using water/ ethanol, and then finally dried under a vacuum atmosphere[39].

The proposed mechanism of palladium complex (C1) preparation is presented in scheme 4 and the 3D structure of Pd-A_1 complex is given in scheme 5.

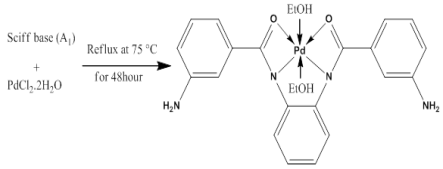

Scheme 4: The proposed mechanism of the synthesis of palladium complex (C1)

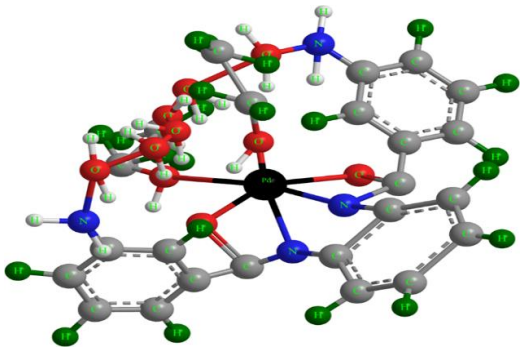

Scheme 5: 3D Structure of Pd complex

2.3.3. Analytical procedure

For separation and determination of palladium, a sample solution containing 0.94×10^{-6} mol/L of Pd(II) was transferred to a 10 ml centrifuge tube. Then, 2 ml of an acetate buffer solution with pH 4, 1.88 $x10^{-6}$ mol/L of A_1, and 1 ml of (0.06 %V/V) TX-114, were added. The solution was made to 10 ml using DDW. The centrifuge tube is then placed in a water bath for 20 mins at 60 °C to reach equilibration. The sample was centrifuged for 10 minutes at 3500 rpm. Then, centrifuge tube was kept for 15 minutes in an ice bath. The TX-114 rich phase will be settled as a spot at the bottom of the centrifuge tube and the aqueous layer above can then easily be removed by aspiration. The TX-114 rich phase was eluted with 3 mol/L HNO_3 and introduced to ICP-OES to measure the concentration of Pd(II). The Separation efficiency of CPE (E %) was calculated in the surfactant-rich phase from the relation:

$$E\ \% = (C_f/C_i)\ x100$$

Where Ci was the initial concentration of the Pd(II) in the mother liquor before CPE and C_f was the concentration of the Pd(II) after CPE in the TX-114 rich phase.

2.4. Analysis Water samples

Several natural water samples, including Nile water, tap water, and seawater, were collected from Al-Mansoura and Marsa-Matrouh cities. Before analysis, the water samples were pre-filtered, the pH was set to 1 by concentrated HCl drops, and they were kept in clean, high-quality plastic containers.

3. Results and discussion

3.1. Method development

ICP OES should be used under the proper circumstances before analyzing both real and standard samples. The optimized parameters of ICP OES are given in **Table 1**.

Table1: Optimal parameters of ICP-OES for determining Pd(II)

RF generator power (kW)	1.2	Pd wavelength (nm)	340.458
Frequency of RF generator (MHz)	40.68	Viewing height (mm)	9
Plasma gas flow rate (l min^{-1})	12	Pump rate (rpm)	15
Auxiliary gas flow rate (l min^{-1})	0.75		
Nebulizer pressure (kPa)	160		

3.2. Characterization

3.2.1-FT-IR spectra

Figure 1 demonstrates the FTIR spectra of the ligand A_1, the Pd-A_1 complex, and the Pd-A_1 complex in the organic layer. **(a-c)**. As was already noted, the amino groups υ (OH) of the alcohol, υ (OH), υ (NH) of azo -hydrazo form, and υ (NH_2) are recognized to the IR of A_1, **Figure 1a**, which exhibits absorption

broadband in the region between 3635 and 3278 cm^{-1}. The υ (CH)-sp3 band is assigned to the band at 2935 cm^{-1}. The broad bands resulting from the creation of the two types of azo and hydrazo structures, as well as the bands between 1730 and 1440 cm^{-1}, are attributed to υ (C=O), υ (C=N), and ν (C=C). The ν (C-N) group is responsible for the band that was shown at 1385 cm^{-1}. Aromatic CH is the reason that bands between 1330 and 736 cm^{-1} appear[40]. The complexation of the ligand with the metal ion is demonstrated by the IR spectra of the Pd (II)-A_1 complex, **Figure 1, b**. It was discovered that there is a considerable shift of the υ (OH), ν (NH), υ (C=N), and υ (C-N), vibrations in the spectra of the free ligand A_1 compared to that of the Pd (II) ion. The fact that the vibrations of υ (C=C) and υ (C=O) are more or less in the same area indicates that (C=C) is not involved in the coordination of the metal ion[41]. As a result, A_1 functions as a neutral bidentate coordination site through the azomethine nitrogen (C=N), (C-N), (C=O), and υ (OH) atoms. Additional evidence for this observation comes from the newly discovered bands at 671 and 436 cm^{-1} and regions attributed to υ (Pd-O) and υ (Pd-N)[42], respectively. The IR spectra of the Pd-A_1 compound in the organic layer, **Figure1, c**, and the Pd-A_1, **Figure1, b**, are comparable, indicating that the CPE process may be physical in nature.

3.2.2-UV-vis spectra

Figure 2 indicates the electronic absorption spectra of A_1 and Pd(II)-A_1 in the aqueous solution and in the TX-114 rich phase. As seen in **Fig2**, the A_1 (**Fig2a**) expresses three absorption bands at 226, 296, and 440 nm, which were determined to be the result of intra-ligand charge transfer (n- π* and π-π*). While the 236, 268, 274, and 510 nm which are the four absorption bands of Pd(II)-A_1 reveal that they were produced by the intraligand charge transfers (n- π* and π-π*) and the ligand-metal charge transfer transitions, respectively. There is a major difference in the absorption spectra of Pd(II)-A_1 in Triton X-114 and the aqueous solution from those of A_1. It is noted that: 1) the Pd(II)-A_1 λ_{max} is red-shifted (at 70 nm) from that of A_1 and 2) Pd(II)-A_1 absorbance in the Triton X-114 system is about four times greater than the absorbance of Pd(II)-A_1 in aqueous solution. The previously mentioned results illustrate that the species are very concentrated in the Triton X-114 layer[42].

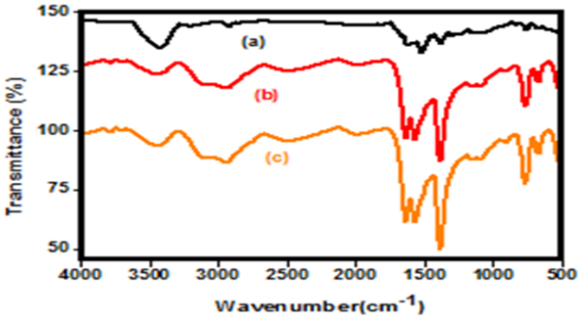

Figure1: The IR spectra of **(a)** the ligand A_1, **(b)** Pd-A_1 complex, **(c)**Pd-A_1 complex in Triton X-114.

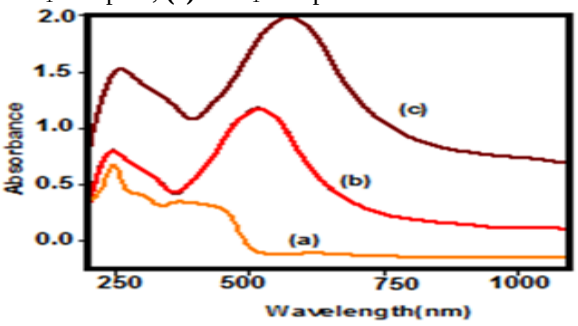

Figure 2: The electronic absorption spectra of **(a)** Schiff base ligand (A_1), **(b)** Pd complex (C1) in aqueous solution and **(c)** Pd -A_1 complex (C1) in Triton X-114

Table2: Analytical and some important physical measurements for A_1 and C1:

C1	**A_1**	**Assignments**	
Refluxing	Refluxing	Preparation Method	
Dark red	Reddish-brown	Color	
Fine crystal	Powder	Aspect	
> 300	174.1	Melting Point (°C)	
48 hours	48 hours	Reaction Time	
86.4	96.5	Yield (%)	
$C_{24}H_{28}N_4O_4Pd$	$C_{24}H_{30}N_4O_4$	Chemical Formula	
3451-3275	3635-3278	ν(OH)-ν(NH) azo hydrazine form	Characteristic infrared frequencies (cm^{-1})
1636	1730	ν(C=O)	
1454	1470	ν(C=N)	
1345	1440	ν(C=C)	
1253	1385	ν(C-N)	
671	---	ν(Pd–O)	
436	---	ν(Pd–N)	
236,268,274,510	226, 296, 440	UV- λ_{max} (nm)	

3.3. CPE-ICP OES determination of Pd(II)

3.3.1. Influence of pH

pH has a vital role in metal–chelation and the production of extractable species from ionic analytes via the Schiff base A_1. The effect of pH on CPE of Pd was studied in the pH range (2 - 10) using 0.94×10^{-6} mol/L with 1.88×10^{-6} mol/L A_1 and 0.06% (v/v) Triton X-114. The results are given in **Figure 3**. Maximum absorbance took place at pH 4, so, pH 4 was selected for further studies. The reduction in absorbance at basic pH was attributed to the precipitation of the analyte ions in the form of hydroxide or may be due to the decomposition of the complex at this pH value [43]. While at a highly acidic pH values(pH<4), the decrease in the absorbance may be due to competition from hydronium ions towards ions for complexation with A_1 and also due to the fact that A_1 is in the non-ionic form at highly acidic media [44]. As it can be noticed, in the absence of A_1(**Figure 3a**), the efficiency of extraction didn't exceed 20%. During the existence of A_1 (**Figure 3b**) cloud point efficiency of Pd(II) readily enhances to nearly 100% around pH 4 and is followed by a reduction in its value. Thus, pH 4 was selected for the following studies.

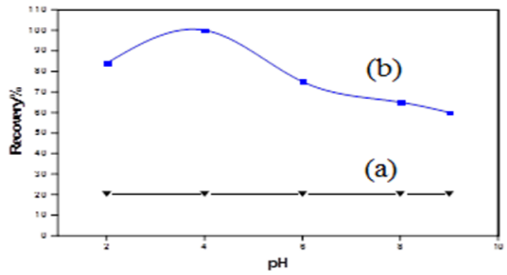

Figure3: Effect of pH on CPE of 0.94×10^{-6} mol/L Pd(II): (a) in the absence; (b) in the presence of Schiff base ligand (A_1), using 0.06% (v/v) TX-114.

3.3.2. Inflence of concentration of A_1 Schiff base ligand and palladium

The CPE efficiency is dependable on the hydrophobicity of the chelating agent (ligand) and the formed complex. Trials of CPE of Pd were conducted by the addition of variable concentrations of A_1 to an appropriate concentration of Pd 0.94×10^{-6} mol/L and 0.06% (v/v) Triton X-114 at pH 4. From the results (**Figure4**), Pd(II) extraction efficiency was increased by increasing A_1 concentration in the range of (0.5-5) $\times 10^{-6}$ mol/L. The maximum extraction efficiency of Pd(II) was found at A_1 (1.88×10^{-6} mol/L) concentration at a ratio of 1:2 (Pd: A_1). Increasing the concentration of A_1 above this level doesn't affect the efficiency of extraction. A finding that can help in the analysis of Pd in samples of unknown concentration. To confirm the previous results, a series of tests were conducted by changing the Pd amount. The obtained data showed that complete extraction occurs at the same previous ratio of 1:2 (M: L). Above such a ratio increasing Pd concentration leads to a decrease in the CPE efficiency.

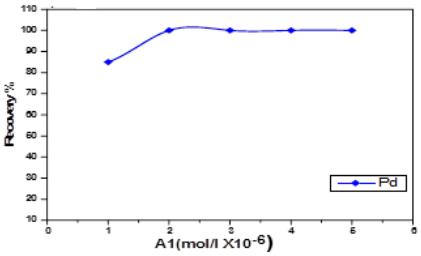

Figure4: Effect of concentration of A_1 Schiff base ligand on CPE of palladium 0.94×10^{-6} mol/L using 0.06% (v/v) TX-114 at pH 4.

3.3.3. Influence of Triton X-114 Concentration:

Triton X-114 was considered because it is commercially available in a highly refined homogeneous form, is inexpensive, and has acceptable toxicological characteristics. Moreover, centrifugation is easily achieved for separation due to the surfactant-rich phase's high density. With all experimental parameters held constant, a variety of concentrations (0.01 -0.1) (v/v) % were applied to examine the influence of Triton X-114 amount on removal efficiency. In (**Figure5**), the findings revealed that at reduced surfactant amount, the separation of the Pd is poor as there are not enough surfactant molecules to isolate the ligand-metal complex quantitatively. The efficiency increases dramatically by raising the surfactant's concentration. The extraction efficiency reaches its maximum value at Triton X-114 concentration of 0.06% (v/v). Hence, 0.06% (v/v) of Triton X-114 was kept constant throughout all subsequent experiments[45].

.

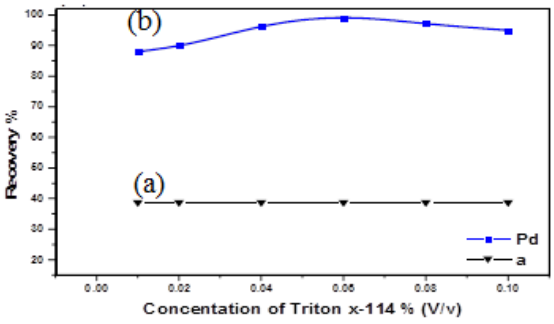

Figure5: Effect of Triton X-114 Concentration on CPE of 0.94×10^{-6} mol/L palladium at pH 4: **(a)** in the absence of A_1 and **(b)** using A_1 (1.88×10^{-6} mol/L).

3.3.4. Influence of different types of surfactants

Several surfactants were used for CPE investigation to pre-concentrate the formed Pd(II) complex (C1). The investigation occurred through the interaction between C1 complex and the hydrophobic surfactant layer. The removal efficiency of the CPE

technique was examined using different types of surfactants as neutral Triton X-100 and Triton X-114, and cationic cetyltrimethylammonium bromide (CTAB). This study proved that CPE of Pd using neutral TX-114 was nearly 100%, while the CPE of Pd by the other surfactants was less than that as shown in **Table 3**. So, Triton X-114 was chosen for this work.

Table3: Effect of different types of surfactants on CPE of palladium using ($0.94x10^{-6}$mol/L analyte at pH4 in the presence of $1.88x10^{-6}$mol/L A_1):

Surfactant	CPE%
	Pd (II)
TX-100	94.0
CTAB	72
TX-100/TX-114/CTAB	94
TX-114	99.7

3.3.5. Influence of the equilibrium temperature and time

The equilibrium temperature parameter was investigated at the range of (20-90°C). The data in (**Figure6 and 7)** shows that the highest recovery was achieved at the range between 60°C and 80°C. After 80 ◦C, the intensity of the signal decreased as the complex will break down at higher temperatures. While the effect of the incubation time was investigated within the range of (5-60 min). It was noted that the incubation time of 20 min is sufficient for the maximum absorbance of analyte ions. The results demonstrate that the incubation time of 20 min and the temperature of 60 °C were selected for further experiments[43].

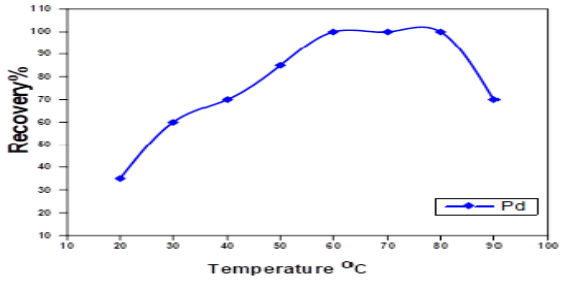

Figure6: Effect of equilibrium temperature on CPE of palladium (0.94×10^{-6} mol/L) using A_1 (1.88×10^{-6} mol/L) and 0.06% (v/v) TX-114 at pH 4.

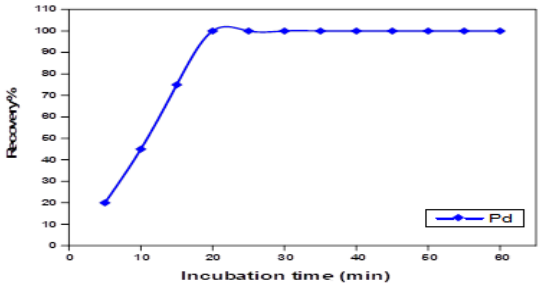

Figure7: Effect of incubation time on CPE of palladium (0.94×10^{-6} mol/L) using A_1 (1.88×10^{-6} mol/L) and 0.06% (v/v) TX-114 at pH 4 at 60ºC**.**

3.3.6. Influence of centrifugation time and rate:

For achieving the optimum separation conditions, the centrifugation time and rate parameters on the Pd(II) extraction recovery were studied. The centrifugation rate and time effects were investigated in the ranges of (500-4000 rpm) and (5-20 min), respectively. After 10 minutes, the surfactant-rich phase was completely separated, **Figure 8**. Accordingly, a centrifugation time of 10 min at 3500 rpm was used in subsequent experiments.

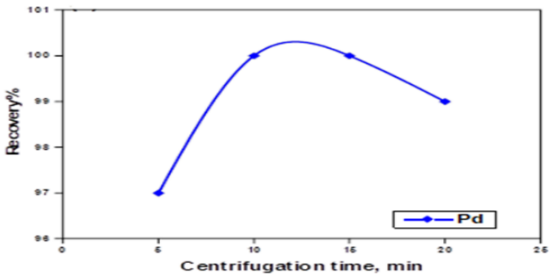

Figure 8: Effect of centrifugation time on CPE of palladium (0.94×10^{-6} mol/L) using A_1 (1.88×10^{-6} mol/L) and 0.06% (v/v) TX-114 at pH 4 at60ºC

3.3.7. Influence of volume:

A series of experiments was carried out to extract a constant concentration of the analyte (0.94×10^{-6} mol/L), from different aqueous volumes using a suitable laboratory tool under the recommended conditions. Hence, different volumes of a water sample 10–250mL and a constant volume of Triton X-114 surfactant 0.06% were chosen. CPE efficiency was not considerably affected up to 100 ml (recovery >95%) and reduced significantly as sample volume increased above 100 ml. The ratio between the initial volume of analyte's solution and the resulting diluted surfactant-rich phase is termed the enrichment factor (preconcentration factor). Accordingly, this study has a preconcentration factor of 100 for the analyte under investigation[46,47].

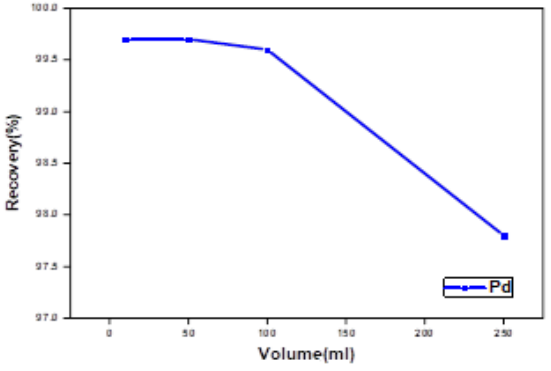

Figure 9: Effect of volume on CPE of palladium (0.94×10^{-6} mol/L) using A_1 (1.88×10^{-6} mol/L) and 0.06% (v/v) TX-114 at pH 4 at 60ºC**.**

3.3.8. Influence of different Elutants

To make it easier to introduce the surfactant-rich phase sample to the ICP-OES nebulizer, the acquired surfactant-rich phase post-isolation should be diluted given that it was highly viscous. Different solvents such as acetone, ethanol, methanol, nitric acid, and acidic solutions (of ethanol and methanol) were examined to select the optimal one according to the signal sensitivity. The reduction of the Pd(II) absorbance signal occurred in presence of the all examined solvents except for HNO_3**.** So, nitric acid of 3 mol/L concentration was used (by applying 3ml).

3.3.9. Influence of added electrolyte

Salt addition is frequently used for ionic strength adjustment as it improves extraction efficiency and reduces the detection limit. The KCL concentration affect the C1 separation that was studied by varying its concentration from 0.01mol/L to 0.1mol/L. It was shown that the C1 extraction efficiency increased with the increasing KCL concentration. The recovery increased with the KCL concentration range from 0.01mol/L to 0.04mol/L, and above the 0.04 mol/L of KCL concentration the recovery decreased. The recovery enhancement may be due to the hydrophobic interaction elevation between the surfactant aggregates and Pd(II) ions. High salt concentrations may cause disturbance to the phases' separation as it leads to an increase in the water drops' density[48].

3.3.10. Influence of foreign ions

According to the ICP-OES high selectivity, the effect of various interferences on the preconcentration procedure was investigated. It occurred through the addition of known amounts of the investigated ions to the aqueous solution containing Pd(II) ions using the proposed methodology. The tolerance level was defined as the maximum amount of foreign species producing an error of ±5% in Pd(II) determination. The results indicate that some metal ions have no considerable effect on the Pd(II) response, while others have acceptable limits of interferences with Pd(II) as shown in **Table4**[49]**.**

Table4: Tolerance limits for the determination of $0.94x10^{-6}$mol/L Pd:

Foreign ions	Concentration (mg/L)	R%
		Pd
Pb^{+2}	5	99
Ni^{+2}	5	97.2
Mn^{+2}	10	98.1
Hg^{+2}	5	96.4
Cr^{+3}	10	98
Cu^{+2}	3	97.9
Fe^{+3}	3	97.3
Co^{+2}	3	98
Na^{+}	230	98.7
CH_3COO^{-}	295	98.4
NO_3^{-}	310	99.5

3.3.11. Analytical characteristics

The calibration graph was linear in the range of 0.1–1 µg/mL under optimum conditions. The calibration equation has a correlation coefficient of 0.9934 and is written as y = 2.6685x+ 0.0426. The limit of detection was 0.02128 µg/L (specified to LOD= 3 SD/m, where SD and m are the blank's standard deviation and calibration curve's slope) The limit of quantification (LOQ) was 0.0636 µg/L (can be calculated as following 3LOD). (c = 5.0 g/ mL, n = 3) The relative standard deviation was 0.022%. **Table5** provides a detailed breakdown of this technique's analytical features[50].

Table 5: The analytical figures of merit of the method

Parameter	Pd (II)
Linear range (µg/mL)	0.1-1
SD	0.01731
RSD % (n=3)	0.022
LOD (µg/L)	0.02128
LOQ(µg/L)	0.0636
Enrichment factor	5
Correlation coefficient	0.9934
Regression equation*	y = 2.6685x + 0.0426
Sample volume (ml)	10

3.3.12. Applications

3.3.12.1. Recovery of Pd(II) in spiked natural water samples

This method's validity and reliability to samples of natural water were investigated by testing the recoveries of some known concentrations of divalent Pd applied to various water samples including doubly distilled, river, and sea samples. The 2, 4, and 6 µg of Pd(II) were added to 20 ml aliquots of filtered water samples, and a dilute acid solution of HCL was used to set the solution's acidity to 4. The scum layer was inserted immediately into ICP-OES for Pd(II) analysis after CPE (as was previously indicated). The recoveries attained ranges from 97.7 to 99.7%. These findings suggest that the detection of trace Pd(II) in actual water samples could be accomplished using this analytical approach.

Table6: Determination of Pd(II) in natural water samples by ICP-OES after using 1.88×10^{-6} mol/L A_1, 0.06%(V/V) Triton X-114 at pH 4.0 at room temperature: (n=5)

Types of water (location)	Spiked (µg/ml)	Measured (µg/ml)	Recovered	Recovery (%)	RSD (%)
Distilled water (Our lab)	0.00	0.00	0.00	0.00	0.00
	2.00	1.991	1.991	99.2	1.41
	4.00	3.952	3.952	98.3	1.32
	6.00	5.935	5.935	97.7	1.21
Tap water (Our lab)	0.00	0.00	0.00	0.00	0.00
	2.00	1.981	1.981	98.4	1.33
	4.00	3.97	3.97	99.3	1.12
	6.00	5.915	5.915	97.9	1.21
Nile water (Mansoura city)	0.00	0.00	0.00	0.00	0.00
	2.00	1.98	1.98	98.2	1.45
	4.00	3.946	3.946	98.8	1.36
	6.00	5.90	5.90	98.9	1.32
Seawater (Marsa Matrouh city)	0.00	0.00	0.00	0.00	0.00
	2.00	1.982	1.982	98.8	1.43
	4.00	3.973	3.973	99.4	1.1
	6.00	5.971	5.971	99.7	0.91

3.3.12.2. Application on synthetic mixtures:

Various synthetic mixtures were prepared using the aqueous sample solution (10ml) of various metal ions, in different proportions and known amounts of Pd**.** Triton X-114 at 0.06% (v/v) and 1.88×10^{-6} mol/L of A_1 were then introduced. ICP-OES was employed to determine the analyte's recoveries with the existence of diverse amounts of interfering ions whereas the CPE strategies were conducted under optimal parameters. Substantial analyte recoveries were reached in all mixes, according to **Table7**'s observations.

Table7: Recovery of Pd (II) ions from chemically synthesized mixtures (n=3) when 1.88 x 10^{-6} mol/L of A_1 was present, at pH 4 and room temperature:

Synthetic mixtures composition (µg/ mL)	Concentration added of Pd (II) (µg/ mL)	Pd (II) (µg /ml)	
		Founded	R %
$Pb^{+2} + Hg^{+2}$	2	1.948	97.4
$Mn^{+2} + Ni^{+2}$	2	1.975	98.75
$Pb^{+2} + Hg^{+2} + Ba^{+2}$	3	2.96	98.67
$Fe^{+3} + Cr^{+3} + Al^{+3}$	3	2.97	99
$Ni^{+2} + Ba^{+2} + Cr^{+3} + Al^{+3}$	4	3.93	98.25
$Ag^{+} + Au^{+2} + Ni^{+2} + Zn^{+2}$	4	3.89	97.25

3.3.13. The plausible Mechanism of the interaction between Triton X-114 surfactant and Pd (II)-A_1 complex

The plausible interaction between Triton X-114 surfactant and Pd(II)-(A_1) complex is schematically represented in **Figure 10**. Triton X-114 surfactant is immiscible with water molecules, which is more favorable for effective separation of Pd(II)-A_1 complex from water. There are also several chemical and physical interactions occurring between Triton X-114 surfactant and Pd(II)-(A_1) complex such as orbital interaction, charge-charge interaction, and hydrogen bond interaction with neutral molecules, van der Waals interaction between alkyl chain, CH-π interaction, π-π interaction, and *n*-π interaction **(Figure 10)**.

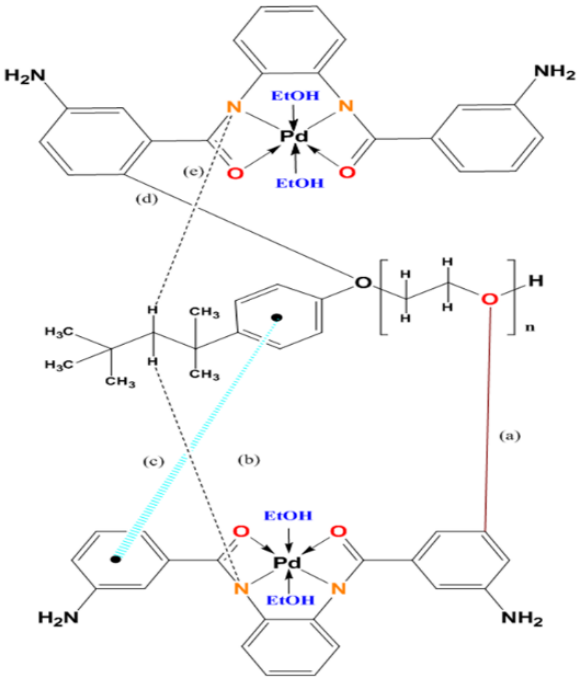

Figure 10: The possible molecular interaction at molecular level
(a, d) O surfactant-H complex interaction
(b, e) H surfactant-N complex interaction
(c) π surfactant-π complex interaction

Table8: Comparative data from some recent studies on preconcentration-separation of palladium ions:

Reagent	Surfactant	Sample volume(mL)	Element	LOD (μgL^{-1})	Sample	Detection	Reference
PAN	Triton X-114	10	Pd	0.4	Water	TLS	[52]
PMBP	PONPE 7.5	10	Pd	1.8	Mine samples	FAAS	[53]
DDA	Triton X-114	10	Pd	0.3	Mine stones &(SRM)	ICP-OES	[54]
A_1	Triton X-114	10	Pd	0.021	Water	ICP-OES	This work

3.3.14. Comparison

A comparison among the existing approach's analytical findings and those of potential alternatives. Table 8 is a summary of the studies that have been reviewed shown to evaluate palladium in past studies. The analytical characteristics of this work were found to be more convenient in comparison with other papers[51].

4. Conclusion

In this paper, a combined CPE -ICP OES methodology was successfully employed separation and determination of ultra-traces of Pd(II) in various aquatic samples using the (N, N'-1, 2-phenylene) bis (3-aminobenzamide) Schiff base (A_1) and the nonionic surfactant Triton X-114. This method was established for the examination of multiple real water samples, and it was successful in recovering more than 95% of the analytes from spiked samples. For the standard spiked samples, the RSD was below 3%. These results demonstrate that this technique is highly repeatable, accurate, and adaptable to compatible samples. The results show that the CPE pre-concentration process is a simple, speedy, precise, adaptable, and sensitive method to extract and pre-concentrate palladium ions.

5. References

1. Malik DS, Sharma AK, Sharma AK, Thakur R, Sharma M. A review on impact of water pollution on freshwater fish species and their aquatic environment. In: Advances in Environmental Pollution Management: Wastewater Impacts and Treatment Technologies. Agro Environ Media - Agriculture and Ennvironmental Science Academy, Haridwar, India; 2020. p. 10–28.
2. FN C, MF M. Factors Affecting Water Pollution: A Review. J Ecosyst Ecography. 2017;07(01).
3. Wang R, Li H, Sun H. Bismuth: Environmental pollution and health effects. In: Encyclopedia of Environmental Health. Elsevier; 2019. p. 415–23.
4. Saleh TA, Mustaqeem M, Khaled M. Water treatment technologies in removing heavy metal ions from wastewater: A review. Vol. 17, Environmental Nanotechnology, Monitoring and Management. Elsevier B.V.; 2022.
5. Al-Jibori AAK, Al-Jibori SAM, Al-Janabi ASM. Palladium(II) and platinum(II) mixed ligand complexes of metronidazole and saccharinate or benzisothiazolinonate ligands, synthesis and spectroscopic investigation. Tikrit Journal of Pure Science [Internet]. 24(6):2019. Available from: http://dx.doi.org/10.25130/tjps.24.2019.105
6. Kandathil V, Kulkarni B, Siddiqa A, Kempasiddaiah M, Sasidhar BS, Patil SA, et al. Immobilized N-Heterocyclic Carbene-Palladium(II) Complex on Graphene Oxide as Efficient and Recyclable Catalyst for Suzuki–Miyaura Cross-Coupling and Reduction of Nitroarenes. Catal Letters. 2020 Feb 1;150(2):384–403.
7. Vojtek M, Marques MPM, Ferreira IMPLVO, Mota-Filipe H, Diniz C. Anticancer activity of palladium-based complexes against triple-negative breast cancer. Vol. 24, Drug Discovery Today. Elsevier Ltd; 2019. p. 1044–58.
8. Cheng H, Chen S, Chen R, Zhou Q. Palladium(II)-Initiated Catellani-Type Reactions. Angewandte Chemie. 2019 Apr 23;131(18):5890–902.
9. Bezerra MA, Ferreira da Mata Cerqueira UM, Ferreira SLC, Novaes CG, Novais FC, Valasques GS, et al. Recent developments in the application of cloud point extraction as procedure for speciation of trace elements. Vol. 57, Applied Spectroscopy Reviews. Taylor and Francis Ltd.; 2022. p. 338–52.
10. Shahryari T, Singh P, Raizada P, Davidyants A, Thangavelu L, Sivamani S, et al. Adsorption properties of Danthron-impregnated carbon nanotubes and their usage for solid phase extraction of heavy metal ions. Colloids Surf A Physicochem Eng Asp. 2022 May 20;641.
11. Ilyas S, Kim H. Recovery of Platinum-Group Metals from an Unconventional Source of Catalytic Converter Using Pressure Cyanide Leaching and Ionic Liquid Extraction. JOM. 2022 Mar 1;74(3):1020–6.
12. Yang Z, Ma J, Liu F, Zhang H, Ma X, He D. Mechanistic insight into pH-dependent adsorption and coprecipitation of chelated heavy metals by in-situ formed iron

(oxy)hydroxides. J Colloid Interface Sci. 2022 Feb 15;608:864–72.
13. Serage AA, Mostafa MM, Akl MA. Low Cost Agro-Residue Derived Biosorbents: Synthesis, Characterization and Application for Removal of Lead Ions ffrom Aqueous Solutions. Egypt J Chem. 2022 Dec 1;65(12):447–61.
14. Akl MA, Hashem MA, Ismail MA, Abdelgalil DA. Novel diaminoguanidine functionalized cellulose: synthesis, characterization, adsorption characteristics and application for ICP-AES determination of copper(II), mercury(II), lead(II) and cadmium(II) from aqueous solutions. BMC Chem. 2022 Dec 1;16(1).
15. Akl MA, Hashem MA, Mostafa AG. Synthesis, characterization, antimicrobial and photocatalytic properties of nano-silver-doped flax fibers. Polymer Bulletin. 2022;
16. Akl MA, El-Zeny AS, Hashem MA, El-Gharkawy ESRH. Synthesis, Characterization and Analytical Applications of Chemically Modified Cellulose for Remediation of Environmental Pollutants. Egypt J Chem. 2021 Jul 1;64(7):3889–901.
17. Mostafa AG, El-Mekbaty A, Hashem MA, Akl MA. Selective separation of Cu(II) from a single metal Ion solution by using O-amino thiophenol-modified flax fiberd. Egypt J Chem. 2021 Apr 1;64(4):1701–8.
18. Saleh MO, Hashem MA, Akl MA. Removal of Hg (II) metal ions from environmental water samples using chemically modified natural sawdust. Egypt J Chem. 2021 Feb 1;64(2):1027–34.
19. Aly HF, Akl MA, A Soliman HM, E AbdEl-Rahman AM, Abd-Elhamid AI. Nano silica particles loaded with CYANEX-921 for removal of iron(III) from phosphoric acid. Vol. 27, Indian Journal of Chemical Technology. 2020.
20. Nayl AA, Abd-Elhamid AI, Abu-Saied MA, El-Shanshory AA, Soliman HMA, Akl MA, et al. A novel method for highly effective removal and determination of binary cationic dyes in aqueous media using a cotton-graphene oxide composite. RSC Adv. 2020 Feb 24;10(13):7791–802.
21. Abd-Elhamid AI, Emran M, El-Sadek MH, El-Shanshory AA, Soliman HMA, Akl MA, et al. Enhanced removal of cationic dye by eco-friendly activated biochar derived from rice straw. Appl Water Sci. 2020 Jan 1;10(1).
22. Abd-Elhamid AI, El Fawal GF, Akl MA. Methylene blue and crystal violet dyes removal (as a binary system) from aqueous solution using local soil clay: Kinetics study and equilibrium isotherms. Egypt J Chem. 2019;62(3):941–54.
23. Shoueir KR, Akl MA, Sarhan AA, Atta AM. New core@shell nanogel based 2-acrylamido-2-methyl-1-propane sulfonic acid for preconcentration of Pb(II) from various water samples. Appl Water Sci. 2017 Nov 1;7(7):3729–40.
24. Shoueir KR, Atta AM, Sarhan AA, Akl MA. Synthesis of monodisperse core shell PVA@P(AMPS-co-NIPAm) nanogels structured for pre-concentration of Fe(III) ions. Environmental Technology (United Kingdom). 2017 Apr 18;38(8):967–78.
25. Sulejmanović J, Memić M, Šehović E, Omanović R, Begić S, Pazalja M, et al. Synthesis of green nano sorbents for simultaneous preconcentration and recovery of heavy metals from water. Chemosphere. 2022 Jun 1;296.
26. Zhai J, Yuan D, Xie X. Ionophore-based ion-selective electrodes: signal transduction and amplification from potentiometry. Sensors & Diagnostics. 2022;1(2):213–21.
27. Akl A M, Bekheit M M. Application of CPE-FAAS Methodology for the Analysis of Trace Heavy Metals in Real Samples using Phenanthraquinone Monophenyl Thiosemicarbazone and Triton X-114. J Anal Bioanal Tech. 2016;7(4).
28. Suham TA, Mohammed SA, Ammash SA. Cloud Point Extraction, Pre Concentration and Spectrophotometric Determination of Nickel and Cad Miumions [Internet]. Vol. 26. 2022. Available from: http://annalsofrscb.ro
29. Akl MA, Ahmad SA. Ion flotation and flame atomic absorption spectrophotometric determination of nickel and cobalt in environmental and pharmaceutical samples using a thiosemicarbazone derivative. Egypt J Chem. 2019;62(10):1917–31.
30. Akl MA, Masoud RAN. Flotation and enhanced spectrophotometric determination of uranium (VI) in environmental samples. Egypt J Chem. 2018;61(2):337–48.
31. Akl MA, Alharwi WSA. AgreenandsimpletechniqueForflotationAndspectrophotometric determination of cobalt(II) in pharmaceutical and water samples. Egypt J Chem. 2018;61(4):639–50.
32. Akl MA, AL-Rabasi AS, Melouk AF. Cloud point extraction and faas determination of copper (II) at trace level in environmental samples using n-benzamido-n'-benzoyl thiocarbamide and ctab. Egypt J Chem. 2021 Jan 1;64(1):313–22.
33. More MS, Joshi PG, Mishra YK, Khanna PK. Metal complexes driven from Schiff bases and semicarbazones for biomedical and allied

applications: a review. Mater Today Chem. 2019 Dec 1;14.
34. Uddin MN, Ahmed SS, Alam SMR. REVIEW: Biomedical applications of Schiff base metal complexes. Vol. 73, Journal of Coordination Chemistry. Taylor and Francis Ltd.; 2020. p. 3109–49.
35. Pervaiz M, Sadiq S, Sadiq A, Younas U, Ashraf A, Saeed Z, et al. Azo-Schiff base derivatives of transition metal complexes as antimicrobial agents. Vol. 447, Coordination Chemistry Reviews. Elsevier B.V.; 2021.
36. Kaur M, Kumar S, Younis SA, Yusuf M, Lee J, Weon S, et al. Post-Synthesis modification of metal-organic frameworks using Schiff base complexes for various catalytic applications. Vol. 423, Chemical Engineering Journal. Elsevier B.V.; 2021.
37. Akl MA, El-Gharkawy ESR, El-Mahdy NA, El-Sheikh SM, Sheta SM. A novel nano copper complex: Potentiometry, DFT and application as a cancer prostatic biomarker for the ultrasensitive detection of human PSA. Dalton Transactions. 2020 Nov 28;49(44):15769–78.
38. Akl MA, El-Mahdy NA, El-Gharkawy ESRH. Design, structural, spectral, DFT and analytical studies of novel nano-palladium schiff base complex. Sci Rep. 2022 Dec 1;12(1).
39. Enamullah M, Al-moktadir Zaman M, Bindu MM, Islam MK, Islam MA. Experimental and theoretical studies on isatin-Schiff bases and their copper(II)-complexes: Syntheses, spectroscopy, tautomerism, redox potentials, EPR, PXRD and DFT/TDDFT. J Mol Struct. 2020 Feb 5;1201.
40. Yao Y, Hou CL, Yang ZS, Ran G, Kang L, Li C, et al. Unusual near infrared (NIR) fluorescent palladium(ii) macrocyclic complexes containing M-C bonds with bioimaging capability. Chem Sci. 2019;10(43):10170–8.
41. Ramesh G, Daravath S, Ganji N, Rambabu A, Venkateswarlu K, Shivaraj. Facile synthesis, structural characterization, DNA binding, incision evaluation, antioxidant and antimicrobial activity studies of Cobalt(II), Nickle(II) and Copper(II) complexes of 3-amino-5-(4-fluorophenyl)isoxazole derivatives. J Mol Struct. 2020 Feb 15;1202.
42. Alkış ME, Buldurun K, Turan N, Alan Y, Yılmaz ÜK, Mantarcı A. Synthesis, characterization, antiproliferative of pyrimidine based ligand and its Ni(II) and Pd(II) complexes and effectiveness of electroporation. J Biomol Struct Dyn. 2022;40(9):4073–83.
43. Roushani M, Mohammad Baghelani Y, Abbasi S, Mohammadi Z. ligandless cloud point extraction of trace amounts of palladium and rhodium in road dust samples using span 80 prior to their determination by flame atomic absorption spectrometry.(2014) Química Nova 37(8)
44. Tavallali H, Malekzadeh H, Karimi MA, Payehghadr M, Deilamy-Rad G, Tabandeh M. Chemically modified multiwalled carbon nanotubes as efficient and selective sorbent for separation and preconcentration of trace amount of Co(II), Cd(II), Pb(II), and Pd(II). Arabian Journal of Chemistry. 2019 Nov 1;12(7):1487–95.
45. Azooz EA, Shabaa GJ, Al-Mulla EAJ. Methodology for preconcentration and determination of silver in aqueous samples using cloud point extraction. Brazilian Journal of Analytical Chemistry. 2021;9(35).
46. Kumar Patil A, Satankar M, Kautkar S, Raj R. Chemical Science Review and Letters Article cs20510191 Cloud Point Extraction: A Novel Approach for Extraction of Bioactive Compounds from Fruit and Vegetable Waste. Chem Sci Rev Lett. 2020(34):324–8.
47. Sheikh R El, Shaltout M, Nabawy K El, Gouda AA. A Green Enrichment Method of Copper, Manganese and Nickel in Water Samples via Cloud Point Extraction. Vol. 7, Iranian Chemical Society Anal. Bioanal. Chem. Res. 2020.
48. Azooz EA, Moslim JR, Jawad SK. Cloud point extraction methodology for separation, extraction and preconcentration of mn (VII) coupled with spectroscopy for determination in different samples. Biochem Cell Arch. 2020;20(1):2641–8.
49. Gavazov KB, Racheva P V., Milcheva NP, Divarova V V., Kiradzhiyska DD, Genç F, et al. Use of a Hydrophobic Azo Dye for the Centrifuge-Less Cloud Point Extraction–Spectrophotometric Determination of Cobalt. Molecules. 2022 Aug 1;27(15).
50. Abdallah AB, Youins AM, El-Kholany MR. Selective separation of uranyl ions from some lanthanide elements using a promising β-enaminoester ligand by cloud point extraction. RSC Adv. 2022 Mar 17;12(14):8520–9.
51. Azooz EA, Moslim JR, Hameed SM, Jawad SK, Al-Mulla EAJ. Aspirin in food samples for separation and micro determination of copper(II) using cloud point extraction/solvation method. Nano Biomed Eng. 2021;13(1):62–71.
52. Tong S, Jia Q, Song N, Zhou W, Duan T, Bao C. Determination of gold(III) and palladium(II) in mine samples by cloud point extraction preconcentration coupled with

flame atomic absorption spectrometry. Microchimica Acta. 2011;172(1):95–102.

53. Yu F, Xi C, He Z, Chen L. Development of cloud point extraction for simultaneous extraction and determination of platinum and palladium using inductively coupled plasma optical emission spectrometry in platinum-palladium spent catalysts. Anal Lett. 2010 Apr;43(6):972–82.

54. Shokoufi N, Shemirani F, Shokoufi M. Laser induced-thermal lens spectrometry after cloud point extraction for the determination of trace amounts of palladium. Spectrochim Acta A Mol Biomol Spectrosc. 2009 Oct 15;74(3):761–6.